



Comparing a Fischer-Tropsch Alternate Fuel to JP-8 and Their 50-50 Blend: Flow and Flame Visualization Results

*Yolanda R. Hicks and Kathleen M. Tacina
Glenn Research Center, Cleveland, Ohio*

NASA STI Program . . . in Profile

Since its founding, NASA has been dedicated to the advancement of aeronautics and space science. The NASA Scientific and Technical Information (STI) program plays a key part in helping NASA maintain this important role.

The NASA STI Program operates under the auspices of the Agency Chief Information Officer. It collects, organizes, provides for archiving, and disseminates NASA's STI. The NASA STI program provides access to the NASA Aeronautics and Space Database and its public interface, the NASA Technical Reports Server, thus providing one of the largest collections of aeronautical and space science STI in the world. Results are published in both non-NASA channels and by NASA in the NASA STI Report Series, which includes the following report types:

- **TECHNICAL PUBLICATION.** Reports of completed research or a major significant phase of research that present the results of NASA programs and include extensive data or theoretical analysis. Includes compilations of significant scientific and technical data and information deemed to be of continuing reference value. NASA counterpart of peer-reviewed formal professional papers but has less stringent limitations on manuscript length and extent of graphic presentations.
- **TECHNICAL MEMORANDUM.** Scientific and technical findings that are preliminary or of specialized interest, e.g., quick release reports, working papers, and bibliographies that contain minimal annotation. Does not contain extensive analysis.
- **CONTRACTOR REPORT.** Scientific and technical findings by NASA-sponsored contractors and grantees.

- **CONFERENCE PUBLICATION.** Collected papers from scientific and technical conferences, symposia, seminars, or other meetings sponsored or cosponsored by NASA.
- **SPECIAL PUBLICATION.** Scientific, technical, or historical information from NASA programs, projects, and missions, often concerned with subjects having substantial public interest.
- **TECHNICAL TRANSLATION.** English-language translations of foreign scientific and technical material pertinent to NASA's mission.

Specialized services also include creating custom thesauri, building customized databases, organizing and publishing research results.

For more information about the NASA STI program, see the following:

- Access the NASA STI program home page at <http://www.sti.nasa.gov>
- E-mail your question to help@sti.nasa.gov
- Fax your question to the NASA STI Information Desk at 443-757-5803
- Phone the NASA STI Information Desk at 443-757-5802
- Write to:
STI Information Desk
NASA Center for AeroSpace Information
7115 Standard Drive
Hanover, MD 21076-1320



Comparing a Fischer-Tropsch Alternate Fuel to JP-8 and Their 50-50 Blend: Flow and Flame Visualization Results

*Yolanda R. Hicks and Kathleen M. Tacina
Glenn Research Center, Cleveland, Ohio*

Prepared for the
Central States Section Spring Technical Meeting
sponsored by the Combustion Institute
Dayton, Ohio, April 22–24, 2012

National Aeronautics and
Space Administration

Glenn Research Center
Cleveland, Ohio 44135

Acknowledgments

This work was supported by the Subsonic Fixed Wing Project in NASA's Aeronautics Research Mission Directorate.

This report is a formal draft or working paper, intended to solicit comments and ideas from a technical peer group.

This report contains preliminary findings, subject to revision as analysis proceeds.

This work was sponsored by the Fundamental Aeronautics Program at the NASA Glenn Research Center.

Level of Review: This material has been technically reviewed by technical management.

Available from

NASA Center for Aerospace Information
7115 Standard Drive
Hanover, MD 21076-1320

National Technical Information Service
5301 Shawnee Road
Alexandria, VA 22312

Available electronically at <http://www.sti.nasa.gov>

Comparing a Fischer-Tropsch Alternate Fuel to JP-8 and Their 50-50 Blend: Flow and Flame Visualization Results

Yolanda R. Hicks and Kathleen M. Tacina
National Aeronautics and Space Administration
Glenn Research Center
Cleveland, Ohio 44135

Abstract

Combustion performance of a Fischer-Tropsch (FT) jet fuel manufactured by Sasol was compared to JP-8 and a 50-50 blend of the two fuels, using the NASA/Woodward 9 point Lean Direct Injector (LDI) in its baseline configuration. The baseline LDI configuration uses 60° axial air-swirlers, whose vanes generate clockwise swirl, in the streamwise sense. For all cases, the fuel-air equivalence ratio was 0.455, and the combustor inlet pressure and pressure drop were 10-bar and 4 percent. The three inlet temperatures used were 828, 728, and 617 K. The objectives of this experiment were to visually compare JP-8 flames with FT flames for gross features. Specifically, we sought to ascertain in a simple way visible luminosity, sooting, and primary flame length of the FT compared to a standard JP grade fuel. We used color video imaging and high-speed imaging to achieve these goals. The flame color provided a way to qualitatively compare soot formation. The length of the luminous signal measured using the high speed camera allowed an assessment of primary flame length. It was determined that the shortest flames resulted from the FT fuel.

1.0 Introduction

Due to the rising cost of oil and the need to supplement the domestic petroleum supply (Refs. 1 and 2), interest in non-petroleum-based jet fuels is increasing. Domestic supplies of coal and natural gas can be converted to jet fuel using the Fischer-Tropsch process (Ref. 3). Fischer-Tropsch fuels have two other advantages when compared to conventional jet fuel: a higher breakpoint (Ref. 4) and lower emissions of particulates (Refs. 1 and 5). Because of these advantages, NASA's Fundamental Aeronautics/Subsonic Fixed Wing (SFW) Project has been sponsoring experiments using Fischer-Tropsch fuels.

For example, the NASA-led Alternative Aviation Fuels Experiment (AAFEX) measured particulate emissions from a DC-8 aircraft with CFM-56-2 engines. The DC-8 was parked on the runway of the NASA aircraft facility in Palmdale, California, and emissions were measured at multiple downstream locations. Emissions were measured with the following fuels: JP-8, a Fischer-Tropsch fuel made from natural gas, a Fischer-Tropsch fuel made from coal, and 50-50 blends of the JP-8 and Fischer-Tropsch fuels. Results showed that the burning the Fischer-Tropsch fuel reduced both volatile and nonvolatile (i.e., soot) emissions, especially at low power and idle conditions (Ref. 1).

The study described here complements the AAFEX campaign. The AAFEX campaign studied emissions downstream of the engine. In contrast, this study uses a flame tube to study conditions in the combustor itself. The AAFEX campaign used a late-1970's technology CFM-56-2 engine with a conventional combustor; this study uses a low-emissions combustor concept similar to what may be used in future aircraft engines.

The low-emissions combustor concept used in this study is the 9-point lean direct injection (LDI) concept (Ref. 6). As the name implies, in LDI the combustor operates fuel-lean without a rich front end: all of the combustor air except that used for liner cooling enters through the combustor dome. Like other lean burn combustor concepts, LDI reduces nitrogen oxides (NO_x) emissions by minimizing flame temperature; in fuel lean combustion, NO_x is an exponential function of temperature. To eliminate local "hot spots" that produce high levels of NO_x , lean burn combustion concepts rely on the fuel and air being well-mixed before burning occurs. Thus, LDI requires rapid fuel vaporization and fuel-air mixing. LDI

achieves this by using a multielement concept in which several small fuel/air mixers replace a single conventional fuel/air mixer. Several LDI geometries have been studied (Refs. 6 to 8); the 9-point LDI geometry used in this study is the baseline geometry described in Reference 6.

Combustion performance of a Fischer-Tropsch jet fuel manufactured by Sasol (designated herein as FT-2) was compared to JP-8 and a 50-50 blend of the two fuels. The objectives of this experiment were to visually compare JP-8 flames with FT-2 flames for gross features. Specifically, we wanted to ascertain in a simple way visible luminosity, sooting, and primary flame length of the FT-2 compared to a standard JP grade fuel. We used video imaging and high-speed imaging to achieve these goals.

2.0 Fuel Composition

JP-8 is a standard, refined aircraft engine fuel. Table 1 shows a typical JP-8 composition. Its constituents fall within the standards for that JP-fuel class, and JP-8 contains up to 20 percent aromatics by volume, many being polycyclic aromatic hydrocarbons (PAH) such as naphthalene (C10). Thus, JP-8 inherently contains soot precursors such as benzene and toluene, and polymerized soot constituents such as the PAH. Table 2 shows a comparison between the specific FT-2 fuel used for testing and a JP-8 sample. The total aromatic content of the FT-2 fuel is only 0.6 volume percent compared to 18.6 for JP-8. The FT-2 fuel also has zero naphthalene and presumably no PAH content. Because the FT-2 aromatic content is low, we expect very little soot formation and lower flame luminosity compared to the JP fuel. The FT-2 is slightly more volatile and has a higher H/C ratio. The higher cetane index for the FT-2 indicates that it has a shorter ignition delay time than does JP-8.

TABLE 1.—TYPICAL FUEL COMPOSITION OF JET-A OR JP-8 (REF. 9)

Components	Volume, percent	Molecular, weight	Boiling pt, °C	Density, g/ml
C8 paraffins	0.3	114.2	118	0.70
C8 cycloparaffins	0.2	112.2	124	0.78
C8 aromatics	0.1	106.2	139	0.87
C9 paraffins	2.4	128.3	142	0.72
C9 cycloparaffins	1.5	126.2	154	0.80
C9 aromatics	1.0	120.2	165	0.88
C10 paraffins	5.6	142.3	160	0.72
C10 cycloparaffins	3.5	140.3	171	0.80
C10 aromatics	2.3	134.2	177	0.86
C11 paraffins	8.7	156.3	196	0.74
C11 cycloparaffins	3.3	154.3	196	0.80
Dicycloparaffins	3.1	152.3	201	0.89
C11 aromatics	3.6	148.2	205	0.86
C12 paraffins	10.8	170.3	216	0.75
C12 cycloparaffins	8.0	166.3	221	0.88
C12 aromatics	4.6	162.3	216	0.86
C13 paraffins	11.5	184.4	235	0.76
C13 cycloparaffins	8.5	182.4	225	0.80
C13 aromatics	4.9	176.6	234	0.87
C14 paraffins	5.9	198.4	254	0.76
C14 cycloparaffins	4.4	192.4	290	0.94
C14 aromatics	2.5	186.3	295	1.03
C15 paraffins	1.4	212.4	271	0.77
C15 cycloparaffins	1.0	206.4	300	0.90
C15 aromatics	0.6	200.4	305	0.95
C16 hydrocarbons	0.2	226.4	287	0.77
Residual hydrocarbons	0.1	202.3	393	1.27

mixture density, 0.81 g/ml; average carbon number, C12; total aromatics, 19.6%

TABLE 2.—COMPARISON OF THE FT-2 FUEL WITH A JP-8 SAMPLE

Fuel	JP-8	FT2
Sulfur (ppm)	1148	22
Olefins (% vol)	0.9	3.8
Aromatics (% vol)	18.6	0.6
Naphthalenes (% vol)	1.6	0
Distillation		
IBP	158	160
10%	176	167
20%	184	170
50%	207	180
90%	248	208
EP	273	231
Residue (% vol)	0.8	1
Loss (% vol)	0.8	0.9
Flash point °C	46	42
API gravity	41.9	54
Specific gravity	0.816	0.763
Freezing point °C	-50	<-80
Viscosity	4.7	3.6
Cetane index	41	51
Hydrogen content (% mass)	13.6	15.1
Heat of combustion (MJ/kg)	43.3	44.1
Fuel H/C ratio	1.88	2.12

3.0 Experimental Setup

The fuel comparison testing was conducted using the lean direct injection (LDI) concept developed by NASA and described in Reference 6. As illustrated in Figure 1, this baseline configuration consists of an air passage that contains a 60° axial swirler, whose vanes generate clockwise (streamwise) swirl. Shortly after the swirler is a converging-diverging venturi section. At the throat of the venturi, the fuel is injected via a simplex atomizer. At the end of the diffusing venturi is the injector dump plane. Figure 2 shows the 3×3, 9-pt LDI hardware used. The LDI elements are spaced on 25.4-mm centers. The hardware was installed in the optically-accessible flame tube illustrated in Figure 3, with the dump plane at the leading edge of the window which spans 38-mm in the axial direction and is 50-mm high.

For all cases, the fuel-air equivalence ratio, ϕ , was 0.455, the combustor inlet pressure and pressure drop was 150-psia and 4 percent. The three inlet temperatures used were 828, 728, and 617 K. These produced nine combinations, as shown in Table 3.

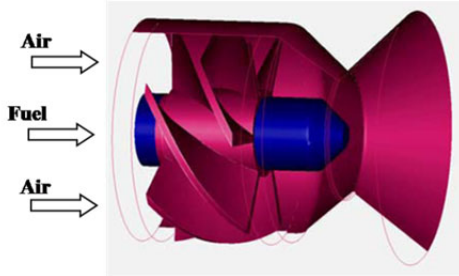


Figure 1.—Schematic drawing that shows the relative spatial positioning of the air swirler, fuel nozzle, and venturi for each LDI injector element.

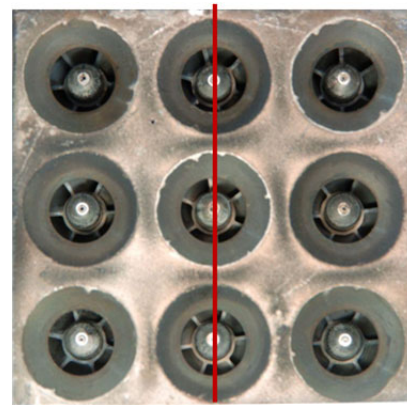


Figure 2.—End view of the 9-point LDI test hardware, with an overlay of the vertical center plane.

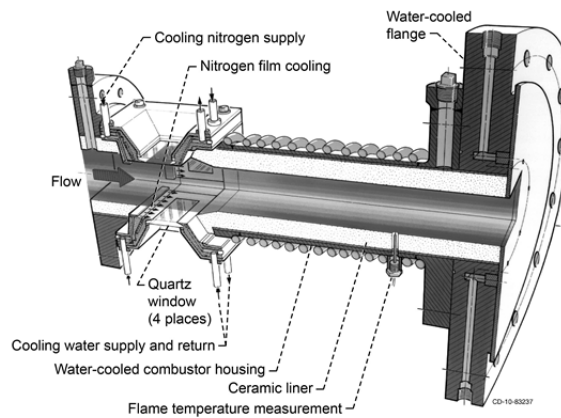


Figure 3.—Schematic drawing of the flame tube combustor used for the LDI alternative fuel test. The injector exit coincides with the upstream edge of the windows.

TABLE 3.—CONDITION MATRIX USED FOR ALTERNATIVE FUEL FLAME IMAGING TEST

JP-8, 828 K	JP-8, 728 K	JP-8, 617 K
50-50 blend, 828 K	50-50 blend, 728 K	50-50 blend, 617 K
FT-2, 828 K	FT-2, 728 K	FT-2, 617 K

The visible flame was recorded in two ways. The first used a standard, 30-Hz, color video camera, having a 1/3-in. format CCD array, focused near the center of the flow. The camera perspective was angled so that multiple injector elements could be seen. For the second imaging technique, we used a 12-bit, grayscale, high-speed camera that has a CMOS array with 1024×1024 pixel resolution. Unlike the video camera, the high-speed camera was set up square to the rig and focused on the imaginary vertical plane that contains the centerline of the middle injector, (overlay in Fig. 2). The high-speed camera frame rate and resolution are variable. The camera can frame as fast as 5400-frames/s (5.4-kps) at full resolution (which provides the maximum field-of view image size), and faster at lower resolutions. For example, to frame at 30-kps requires a reduction in the total number of pixels (and viewable area) read out per image—we used a resolution of 448×384 pixels. For these fuel comparison tests, we collected images with frame rates from 5.4 to 72-kps, with 30-kps typical. The flame chemiluminescence was collected using an $f = 150$ -mm, $f/1.2$ lens. We used three light filtering options, as described in Table 4. These filters were used to reduce the amount of light collected to help optimize image exposure. The filter options were: (1) none, in which all visible light that the camera array is sensitive to was collected; (2) a filter with optical density 2 (OD2), which transmitted one percent of the light; or (3) a combination of an OD1 filter (10 percent transmission) combined with a 473-nm long pass filter. The long pass filter blocked primarily CH* chemiluminescence and allowed most of the C₂* Swann band emissions to pass.

Regardless of the imaging scheme used, all images are volume-based, line-of-sight images, meaning that the total intensity recorded comes from the entire combustor volume that is within the field of view.

TABLE 4.—OPTICAL CHARACTERISTICS OF THE FILTERS USED FOR HIGH SPEED FLAME IMAGING

Filter option	Wavelength band	Transmission, percent
1. None	Visible light	100
2. Neutral density with OD2	Visible light	1
3. Neutral density OD1 and long pass	Visible light longer than 473-nm	10

4.0 Results

4.1 Standard Video Results

We used color video to get a sense of which major constituents were emitting (Ref. 10). In the visible region, emissions in the violet come mainly from CH*, near 432-nm. The other primary chemical species that emits is C₂*, with Swan bands in the blue (473-nm), green (516-nm), and yellow (573-nm). The CH* and C₂* emissions are what we typically consider as the “clean” hydrocarbon flame colors, while orange generally indicates a sooty flame. Soot can be a problem because it detrimentally affects heat transfer to engine subcomponents. Also, particles that are not burnt off before leaving the combustor will carry on through the engine and be exhausted into the atmosphere.

Whether soot is the predominant visible light emitter, we can discern qualitatively by observing the flame color via standard video. Video image results are displayed in Figure 4. The camera was angled so that parts of five LDI elements can be seen. Flow passes from left to right. JP–8 images are in the top row of Figure 4, FT–2 in the bottom row and the blend is shown in the center. The inlet temperature decreases from left column to right. One expected trend for JP–8 is that as the inlet temperature drops, the flame goes from primarily blue-green to primarily yellowish, and there is more soot formation at lower T₃. Light emitted by the soot at the lower temperatures is bright enough to saturate, preventing any real detail from being seen. We also note that even at the highest inlet temperature there is some indication of soot, though the dominant emissions are from the C₂ and CH bond breakage. In comparison, the FT–2 flame is much bluer, with very little soot luminescence. The inlet temperature trend for FT–2 follows that for JP–8, but with much less luminosity from soot. These results are reasonable given the fuel constituent comparison in Table 2, in which we see that the FT–2 contains only 0.6 percent aromatics.

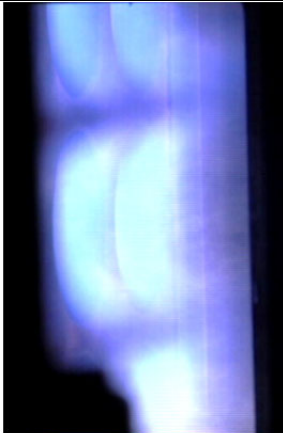
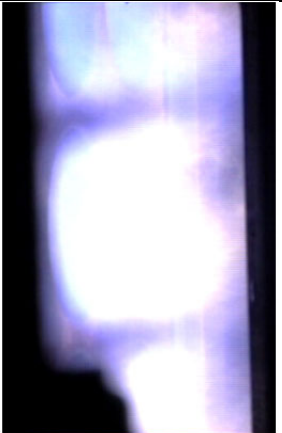

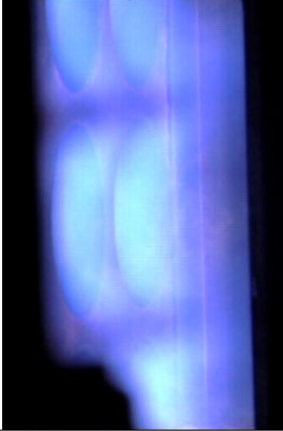
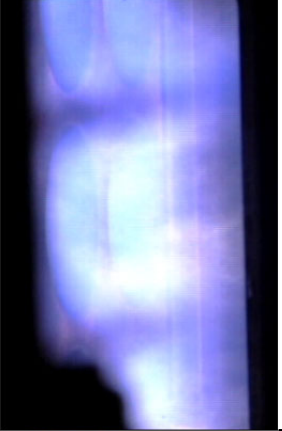

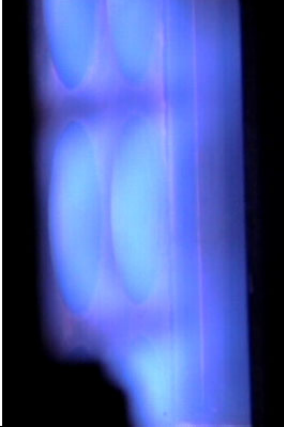


Fuel Type ↓	T_{inlet} →	828 K	728 K	617 K
JP8				
50-50 Blend				
FT-2				

Figure 4.—Standard video images, with flow from left to right. The flow field is partially blocked in the lower left corner by other test rig instrumentation.

In general, we can see distinct flames from each injector element that appear to begin burning before exiting the diffuser. We cannot discern any sort of angle, or flare, to the flame, nor can we determine the length of the primary zone. For that information, we turn to the high speed digital camera.

4.2 High Speed Image Results

Figures 5 and 6 each show ten consecutive frames from the high speed camera for the 828 and 728 K inlet temperature cases. The frame rates are 12 and 30-kps, respectively. Exposure time per image is $1/(\text{frame rate})$. Flow passes from left to right. These snapshots suggest a rapidly varying, turbulent flow. For each case, it appears that the downstream extent of the visible light emitted is slightly greater for the JP-8 case than for the alternative fuel.

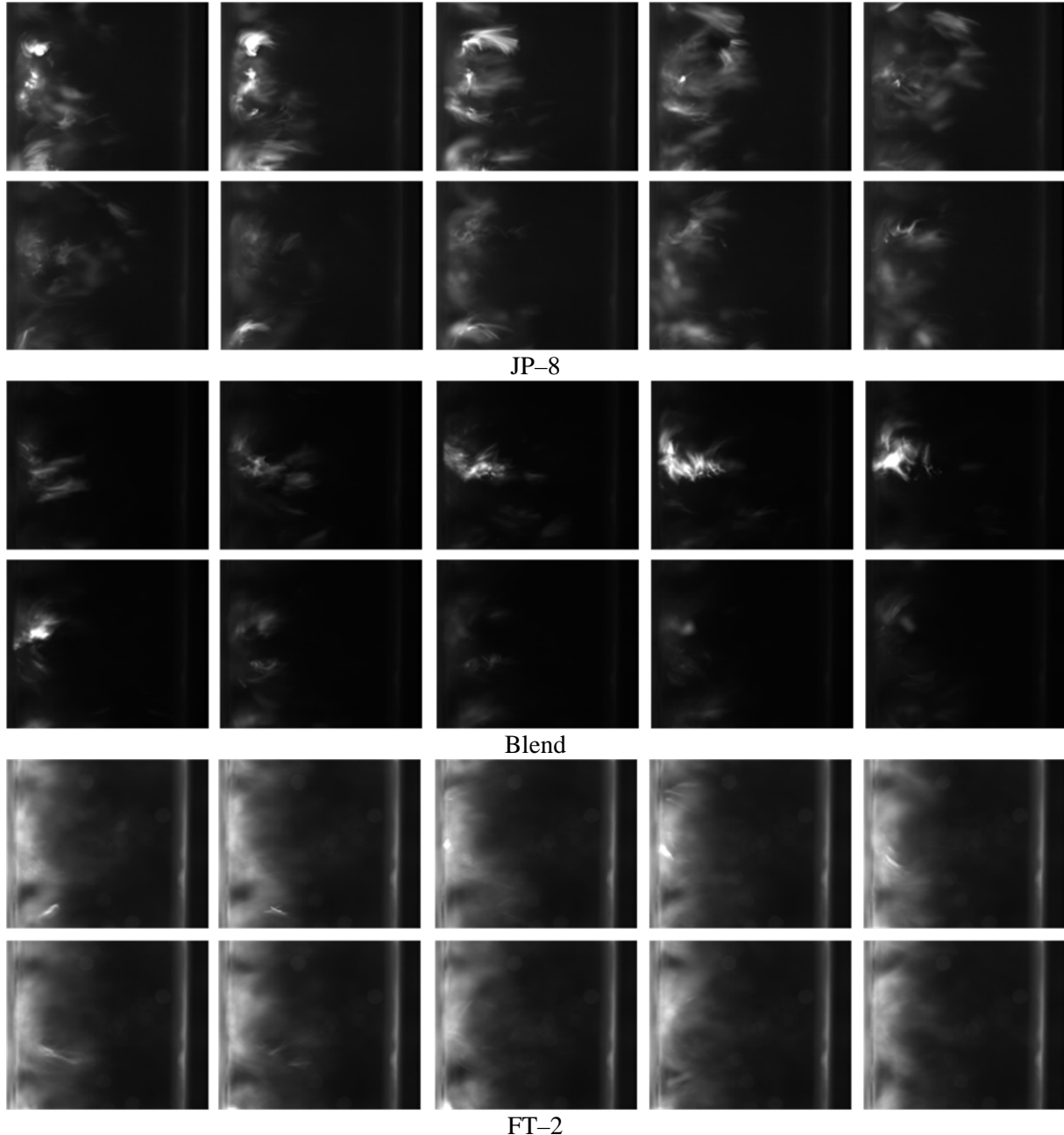


Figure 5.—Ten successive images at $T_3 = 828$ K framed at 12 kps that show flames burning JP-8 (top), the 50-50 blend (center) and FT-2. The top and center images are filtered using an optical density of 1 so as to avoid image saturation. The bottom images are unfiltered because the exposure is inadequate (too dim) with OD1. Image resolution and framing is such that the center row is fully captured, plus a bit from the rows above and below. The downstream window edge is visible on the right as a vertical line. Flow passes from left to right.

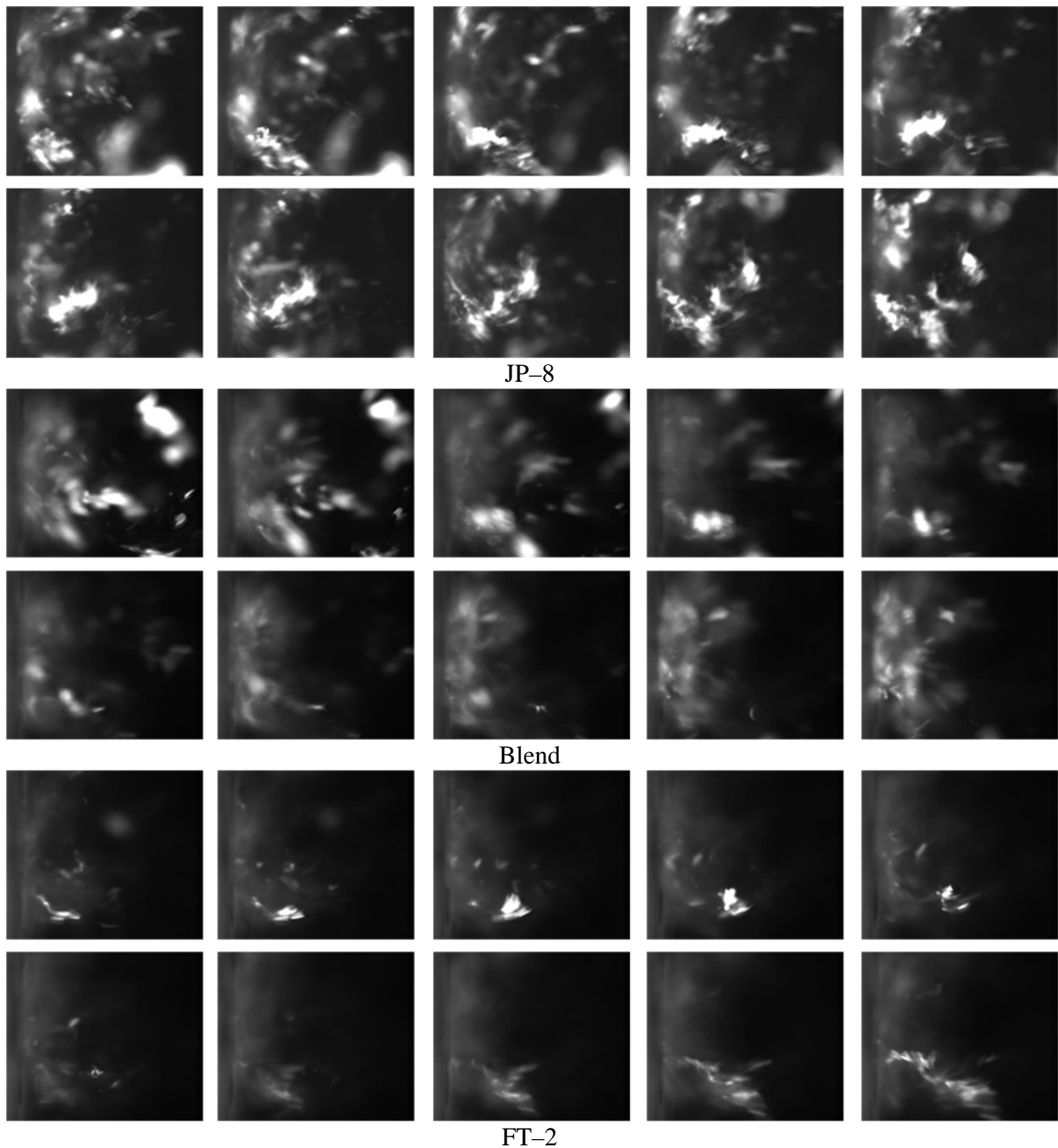


Figure 6.—Ten successive frames at $T_3 = 728$ K framed at 30 kps that show flames burning JP-8 (top), the 50-50 blend (center) and FT-2. All images are unfiltered. The framing captures the flame from the center row of injectors and extends approximately 26-mm downstream. Flow passes from left to right.

The frame rate of 12-kps provides a pixel resolution (748×640) such that one can observe fully the center row plus parts of the adjacent top and bottom rows. The downstream window edge can also be seen in these images as a relatively bright (compared to its surroundings), vertical line. This frame rate is also slow enough that some individual images appear to have “wisps” or streaks of flame visible. This streakiness suggests that the fluid is moving faster than the 83- μ s exposure time of the frames, and we are able to track to some extent “flamelets.” The exposure time is also long enough that the filter set with optical density 1 (which transmitted 10 percent of the incident light longer than 473-nm) was required for the pure JP-8 and the 50-50 blend so as to avoid excessive image saturation. The FT-2 case did not emit

as much light, and no filter was used. Filter usage was therefore consistent with our observations of flame luminosity from the video camera. Also using this resolution and the FT-2 image set, one can get some sense of the overall spray/flame shape or boundary.

There are fewer streaks in the 30-kps image sequences, so this exposure time does a better job of stopping fluid motion within each frame. The resolution for these images, at 448×384 pixels, was just enough to capture the center row of injectors. Because the 30-kps images shown were obtained without filters, we can again qualitatively say that the FT-2 fuel emits less visible light than does the JP-8 when burning.

Using the visible luminescence, we examine these flames for structure, length and interaction between adjacent rows. Figure 7 shows the average luminous intensity and flame shape for the images framed at 12-kps (the images in Figure 5 are subsets of the images used to determine the averages). Each image is scaled independently. Flow passes from left to right. The y-axis scale shows vertical distance from the centerline of the 9-point injector array; the x-axis scale is the distance from the injector dump plane (diffuser exit). There is also an overlay on each image of a dashed, white, line that represents the approximate vertical center of the injector array. For all cases, we note that the center row is relatively self-contained, with little interaction between adjacent rows, as evidenced by the relatively low signal between the rows. The signal about the “centerline” is slightly asymmetric, with the higher signal in the upper half. This asymmetry might be related to interactions induced by the air swirl (all co-rotating) of adjacent injectors (and is a topic outside the scope of this paper). The key differences between fuel types highlighted by the Figure 7 images are the shape of the luminous structure and its distance from the injector exit. For JP-8, the central structure has a slight flare above and below from which one might infer a short, conical shape. For the blend and the FT-2, the structure is more rectangular. We also observe that the primary heat release shifts closer to the dome for the FT-2. The average shape is such that one might speculate that the structure we see for the JP-8 has shifted upstream into the diffuser when burning the alternative fuel. That is, if we take the observed JP-8 signal and simply shift it upstream, is there a point where we would likely see a field similar to that for FT-2?

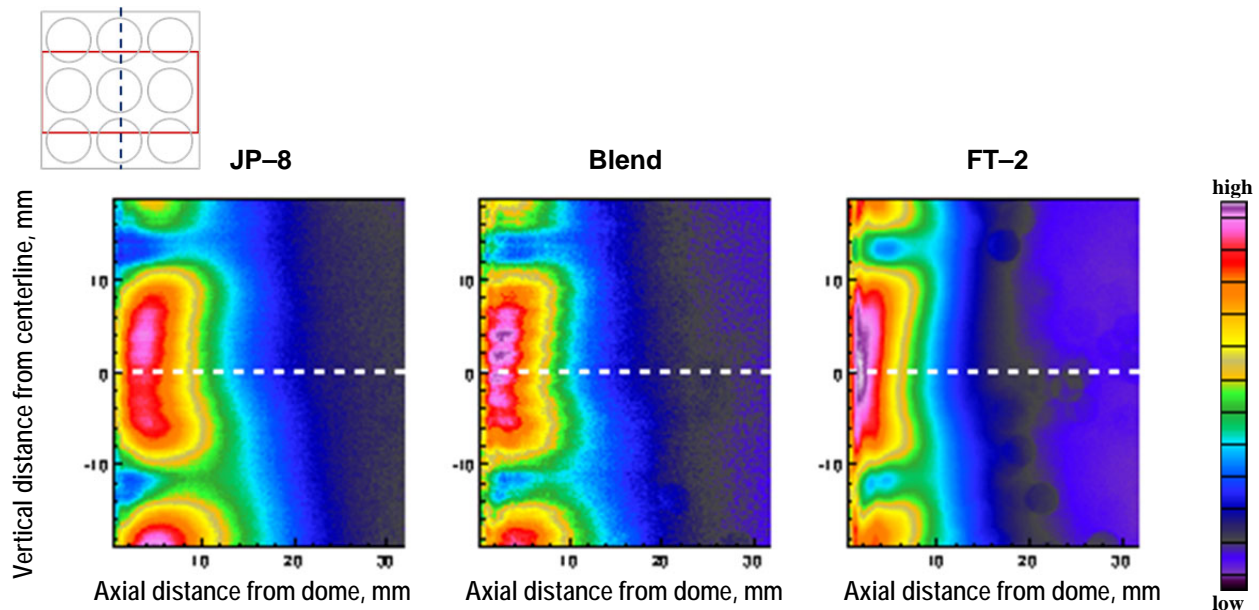


Figure 7.—Average flame structure and luminous intensity obtained by averaging over 6000 frames for the $T_3 = 828$ K cases. Flow is from left to right. The frame rate was 12000 fps. As illustrated by the rectangular overlay in the above cartoon, framing fully incorporates the center row, plus part of the top and bottom rows. The axial span shown is approximately 0 to 30 mm downstream from the injector exit.

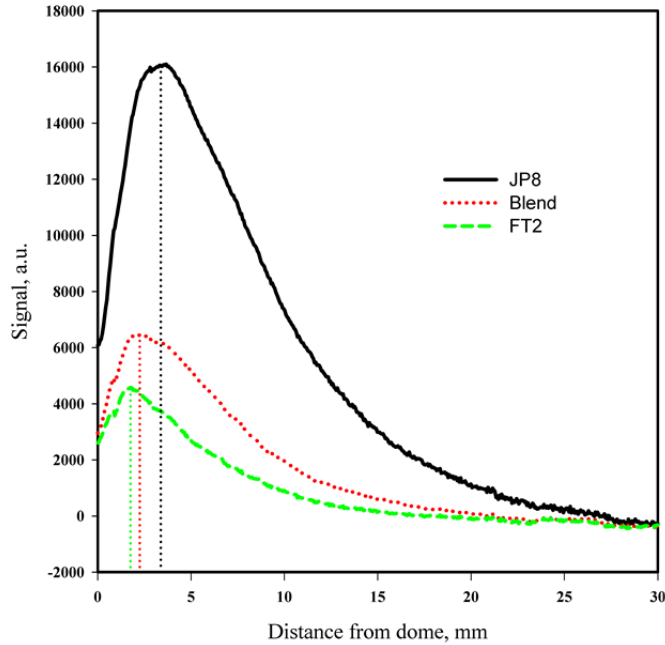


Figure 8.—Comparison showing average flame length and luminous intensity for $T_3 = 828$ K, for a 0.6-mm horizontal strip around the vertical center of the images shown in Figure 7. The frame rate was 12 kps.

Figure 8 presents the signal for the 0.6-mm high horizontal strip through the center row of the Figure 7 images along the dashed line. The drop lines show the location of peak signal. Although the vertical scale has arbitrary units, the values reflect the relative maximum intensities, as they have been corrected based on the filter used. Assuming the intensity reflects the core flame length, we determine from this plot that the FT-2 fuel burns closer to the injector exit, with a peak location about 2-mm away, compared to 4-mm for JP-8. This result makes sense because the FT fuel vaporizes more easily, has a higher cetane index (which is an indicator of shorter ignition delay time) and also has a greater hydrogen and olefin content compared to the JP fuel, both of which are indicators of a more easily reactive fuel.

Because aromatics tend to have longer ignition delay times, the aromatic components of the fuels will tend to burn farther downstream than will the saturated hydrocarbons. The aromatics will also produce the most soot, and the areas of the flame with the most soot will produce the highest signal levels. Both these characteristics are reflected in Figure 8. Another way to consider this is by computing histograms of the signal in the images.

Figure 9 shows histograms for jet fuel and for FT-2 for the middle inlet temperature case (728 K), and all were made from 30,000 fps images. Each histogram is for one pixel; this pixel is located vertically on the image centerline and horizontally at the axial distance stated on the histogram (2.5, 5.0, 7.5, 10.0, or 15.0 mm). The x-axis of these histograms represents a bin for each possible signal value (0 to 4095), and the y-axis gives the percentage of images where the pixel of interest is at that level. The solid vertical line marks the mean at that pixel, and the dashed vertical line marks the median. The left column shows histograms for JP-8 fuel. These histograms result from the images taken with the third filter listed in Table 4: OD1 with a 473-nm long-pass filter. The right column shows histograms for Fischer-Tropsch fuel obtained without a filter. It was not possible to perform a good comparison using the same filtering for both fuels because the unfiltered images for JP-8 saturated too much (20 percent of the time); whereas the images obtained using filter set 3 for the FT-2 were quite dim and did not make full use of the dynamic range available (the mean value was always less than 200 counts, with a maximum less than 500 counts). All images in an image set were used to construct the histograms: 5,388 images for the JP-8 histograms and 5,073 images for the unfiltered alternative fuel histograms.

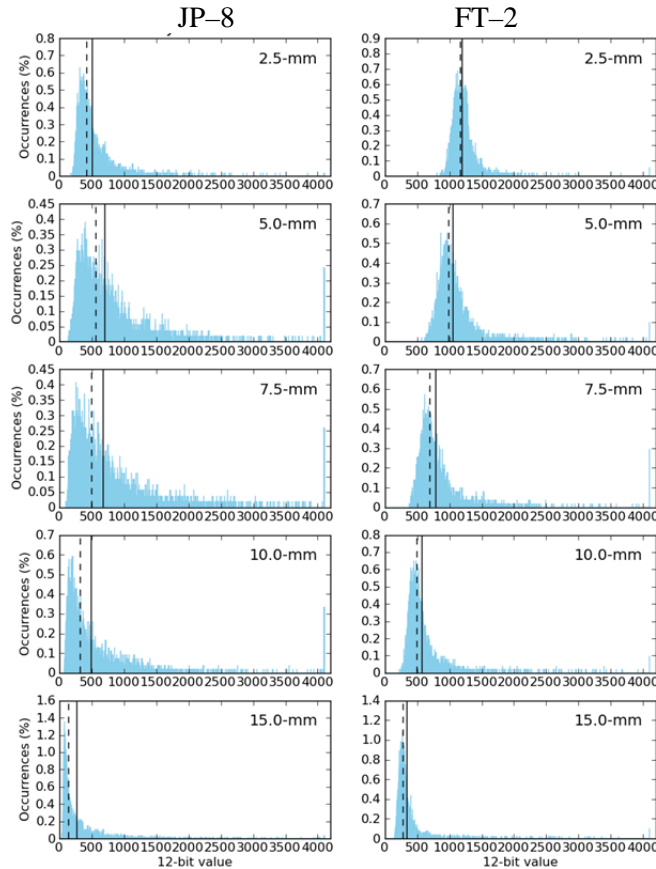


Figure 9.—Histograms derived from 30,000 fps high speed movies for JP-8 with filter 3 (left column) and unfiltered FT-2 (right). The histograms show the percent of occurrences of light signal level for a single pixel that lies along the vertical midpoint of the middle injector row (the relative “centerline”) at the downstream distances indicated. The inlet temperature was 728 K.

The JP-8 and FT-2 histograms show some similarities. All distributions are unsymmetrical, with longer tails at higher signal levels than at lower signal levels. For this reason, the mean is always higher than the median. For both the JP-8 and the unfiltered FT-2 case, the distribution becomes more skewed towards higher signal levels as the downstream distance increases. In particular, the peak in the number of saturated (4095) values is downstream of the location where the mean peaks. For this reason, the ratio of the mean to the median tends to increase with downstream distance. The increased skew towards higher signal levels at farther downstream distances is consistent with the aromatic components of the fuel burning farther downstream.

Despite these similarities, the JP-8 histograms can easily be distinguished from the FT-2 histograms. First, note that the JP-8 histograms show a wider distribution of signal levels than do the unfiltered alternative fuel histograms despite the fact that the mean value of the alternative fuel histogram is always wider. Second, note that skew towards higher signal levels noted above is more pronounced for the JP-8 histograms. In particular, despite lower means, the peak percentage of saturated values is higher for the JP-8 case (0.33 percent at 10.0-mm) than for the unfiltered FT-2 case (0.30 percent at 7.5 mm). Again, the wider signal distribution, coupled with the more pronounced skew toward higher signal is consistent with the greater aromatic content in JP-8.

As seen in the individual images (Figs. 5 and 6), there is a considerable amount of variation from one image to the next. Figure 10 shows the mean, standard deviation, and span per pixel for the JP-8 (top row) and FT-2 (bottom row) cases. As one might expect, most of the signal variation occurs immediately downstream from the fuel injection region, as shown by the standard deviation, with very little change at all in the areas at the dome face that are between the injection sites. The standard deviation plots also indicate that there is some communication between injectors just a short way downstream. The plots that show the local pixel span also serve to highlight variation from the mean. In this case, they also show a dead zone upstream. They also show that although the flames are short on average, there are occasional excursions to high signal downstream of the primary flame zone.

Figure 11 shows the 30-kps average results for all cases except the JP-8 high T_3 condition. The frame rate allows us to visualize only the center row. As we saw earlier in Figure 7, the high inlet case has higher signal in the upper half of the flame (left column), but the structure and distribution of signal changes as the inlet temperature decreases. In all cases the flame length increases. For FT-2, the structure shifts from a slightly top-heavy asymmetry at 828 K to symmetric at 728 K to bottom-heavy asymmetry at 617 K. In fact, at the lowest temperature the chemiluminescent structure is the same regardless of the fuel used, though the FT-2 peaks closer to the dome. This similarity in structure at 617 K may be because fuel vaporization or reaction rates are closer among the three fuel mixtures than they are at higher temperatures.

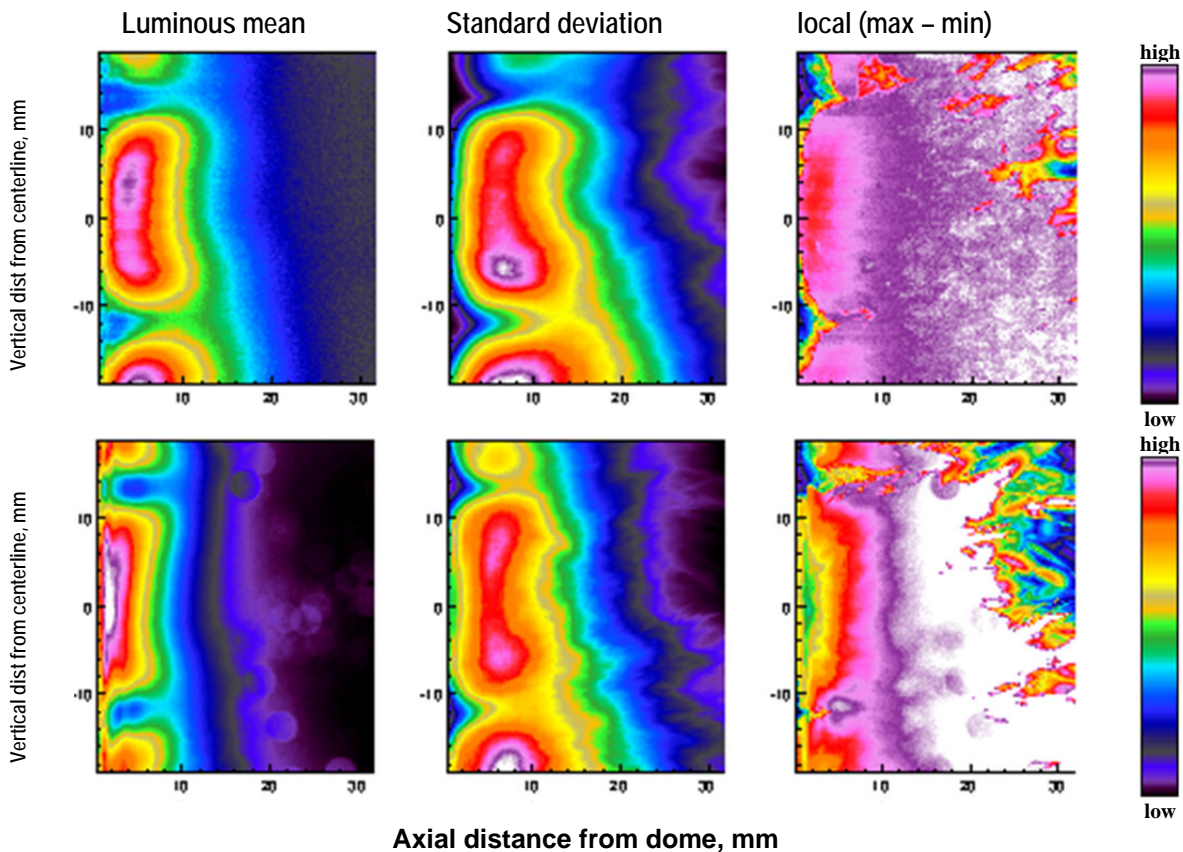


Figure 10.—Statistics derived from processing the signal intensities of over 10000 consecutive flame images on a pixel-per-pixel basis. The camera frame rate was 12,000/s. Inlet conditions: $T = 828$ K, $P = 1034$ -kPa, $\phi = 0.45$, flow left to right. Top row: JP-8; Bottom row: FT-2.

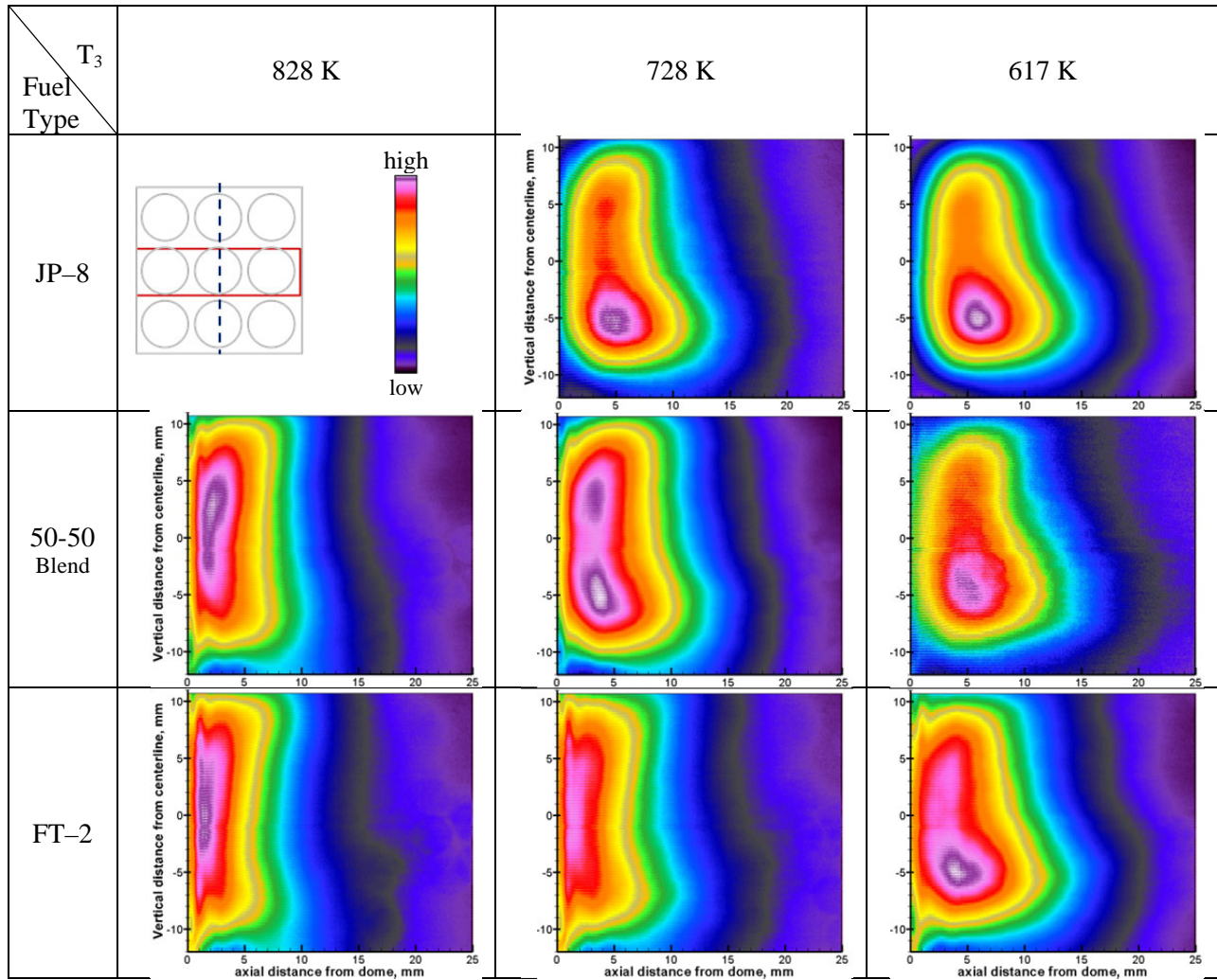


Figure 11.—Average flame structure and luminous intensity obtained by averaging individual movie frames. Each image is independently scaled. The frame rate was 30000/s. The image set for JP-8 at the highest inlet temperature was not adequate for comparison. The end view cartoon shows that framing is about the center row of injectors. The axial distance extends from the dump plane to approximately 25-mm downstream from the injector exit. The height is approximately 23-mm.

Figure 12 shows the resultant fields when the same raw images used to produce the Figure 11 images are processed in a manner similar to particle image velocimetry, so as to track the relative bulk motion of this fluid system. The sets chosen for processing are those that had subjectively good exposures: that is, the images did not saturate too much, and were not too dim. Since the process attempts to correlate the motion from frame to frame, exposure is important and will play a role in the results generated using this procedure; thus these vector results are purely qualitative. Another factor to consider when looking at these plots is that the raw images collected the light transmitted through the bulk of the fluid of a three-dimensional field integrated onto a two-dimensional array. The vectors show the bulk direction of travel; the contours reflect the rate of change for that region of the space.

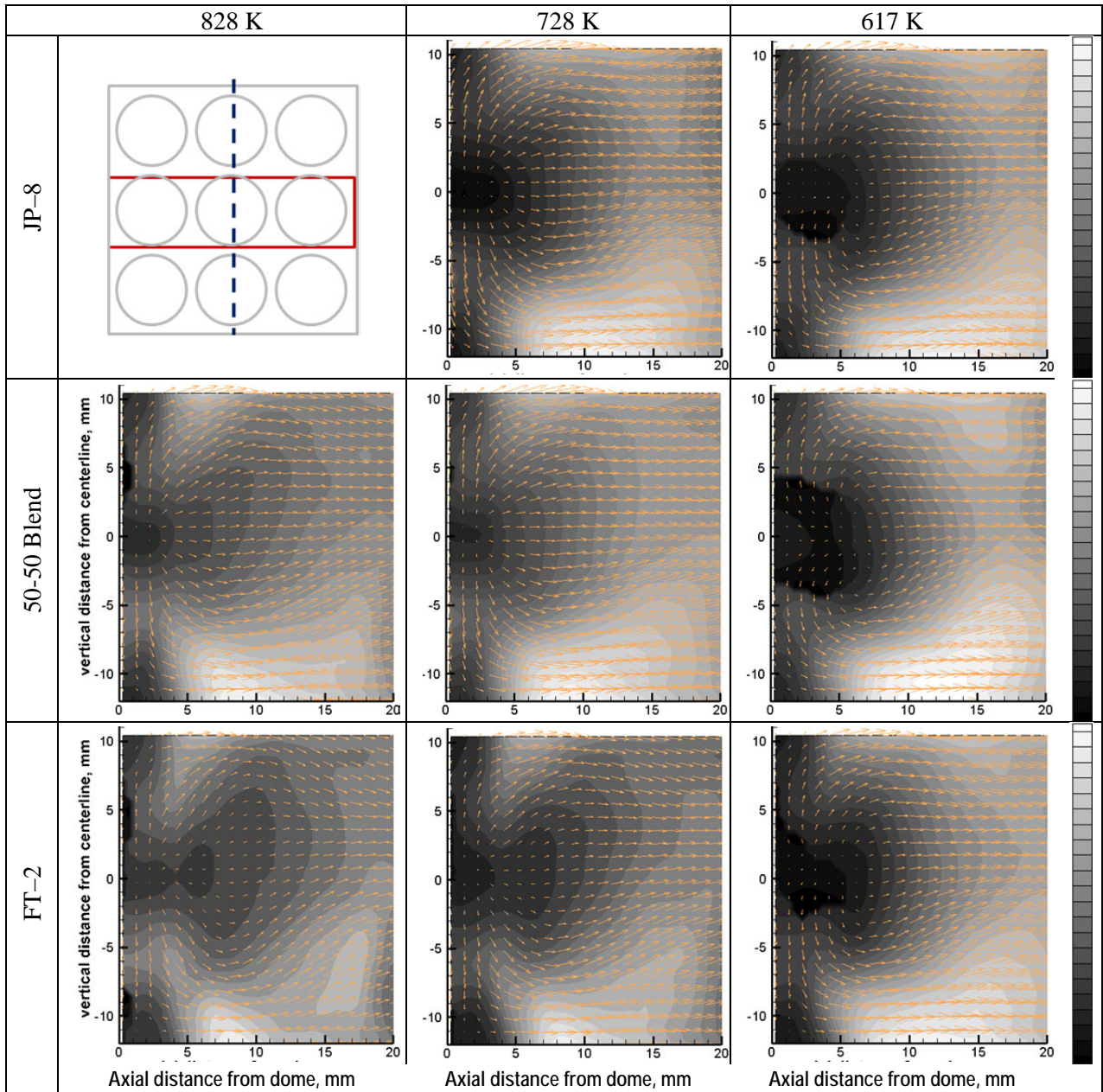


Figure 12.—Average flame zone structure obtained by processing the 5001 consecutive movie frames. The frame rate was 30,000 fps. Framing is about the center row of injectors. The contour denotes the relative magnitude of change within the primary flame zone and the arrows can be interpreted as showing the average direction of motion within the flame zone.

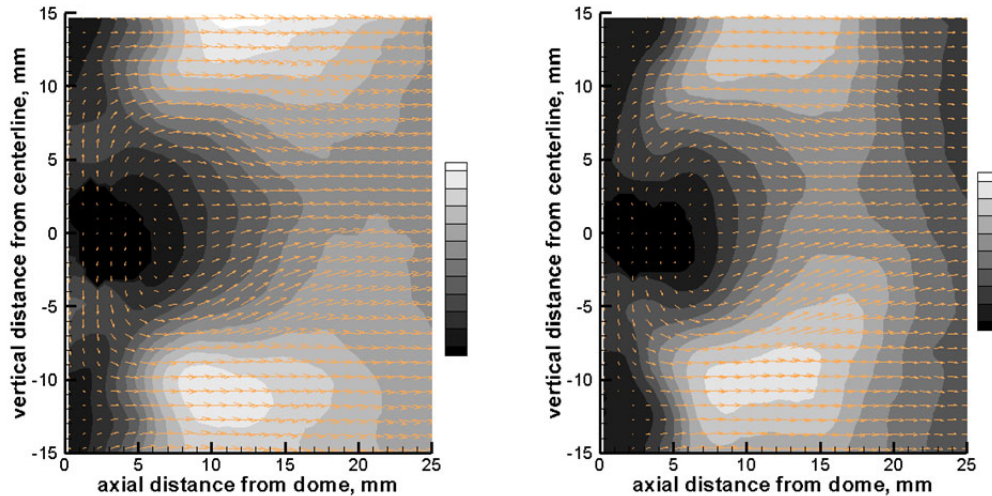


Figure 13.—Average flame zone structure obtained by processing movie frames for JP-8 (left) and FT-2 (right) at inlet temperature 617 K. The frame rate was 16,000 fps. Framing is about the center row of injectors. The contour denotes the relative magnitude of change within the primary flame zone and the arrows can be interpreted as showing the average direction of motion within the flame zone.

The vectors show that the fluid flows radially outward from the injector exit, providing the best evidence that the flow from the injector is conical, regardless of fuel type. The slowest relative motion is immediately downstream, along the injector centerline. These averages show that the greatest change per unit time occurs in the lower half in all cases. This is unlike the case of the chemiluminescence-based averages, which had a shift in intensity from the upper half to the lower half as the inlet temperature decreased. The second greatest area of change is on the mirror opposite side. These areas are where the flow from adjacent injectors downstream is most likely to interact. This can be seen more clearly in the images shown in Figure 13, which compares the two pure fuel cases at the lowest inlet temperature, 617 K, for high speed movies captured at 16,000 fps and the larger field of view that enables one to observe the region between injector rows.

5.0 Concluding Remarks

Using the NASA-developed LDI injector and an optically-accessible flame tube, we visually compared combustion of JP-8, FT-2 and a 50-50 blend of the fuels using standard color video and high speed imaging to examine flame structure. We determined that these simple imaging tools allow one to quickly assess luminosity, soot and flame length. We used the video primarily to assess the “cleanliness” of the flames by considering the flame color. We saw that the JP-8 flames are more likely to soot and that both fuels show more incandescence from soot at the lowest inlet temperature. The high speed camera allowed us to examine the flame structure. We determined that the more reactive FT-2 fuel produces a shorter flame, consistent with the physical properties of that fuel; and that for both fuels the core flame length increased with a lower inlet temperature. In the cases with FT-2, it also seemed that the onset of burning may have moved upstream, into the diffuser area of the injector.

For lower inlet temperature applications, there may not be much improvement in combustion performance when burning the alternative fuel, based on the images. Gas emissions would be needed to make a more complete assessment.

References

1. B.E. Anderson et al, NASA/TM—2001-217059, 2001.
2. P.A. Muzzell, E.R. Sattler, A. Terry, B.J. McKay, R.L. Freerks, L.L. Stavinoho, SAE 2006-01-0702, 2006.
3. M.E. Dry, H.B. de W. Erasmus, *Annual Review of Energy*, 1987.
4. J.S. Klettlinger, A. Surgenor, and C. Yen, NASA/TM—2010-216370, 2010.
5. M.T. Timko et al., *Energy and Fuels*, 24 (2010) 5883-5896.
6. R. Tacina, P. Lee, C. Wey, ISABE-2005-1106.
7. R. Tacina, C.-P.Mao, C. Wey, AIAA-2004-0135, Reno, NV, 2004.
8. R. Tacina, C. Wey, P. Laing, A.A. Mansour, NASA/TM—2002-211347.
9. H.J. Clewell III, *J. Aircraft*, 20 (1983), 382–384.
10. A.G. Gaydon, *The Spectroscopy of Flames*, 2nd Edition, John Wiley and Sons, New York, NY, 1974.

REPORT DOCUMENTATION PAGE			Form Approved OMB No. 0704-0188		
<p>The public reporting burden for this collection of information is estimated to average 1 hour per response, including the time for reviewing instructions, searching existing data sources, gathering and maintaining the data needed, and completing and reviewing the collection of information. Send comments regarding this burden estimate or any other aspect of this collection of information, including suggestions for reducing this burden, to Department of Defense, Washington Headquarters Services, Directorate for Information Operations and Reports (0704-0188), 1215 Jefferson Davis Highway, Suite 1204, Arlington, VA 22202-4302. Respondents should be aware that notwithstanding any other provision of law, no person shall be subject to any penalty for failing to comply with a collection of information if it does not display a currently valid OMB control number.</p> <p>PLEASE DO NOT RETURN YOUR FORM TO THE ABOVE ADDRESS.</p>					
1. REPORT DATE (DD-MM-YYYY) 01-07-2013		2. REPORT TYPE Technical Memorandum		3. DATES COVERED (From - To)	
4. TITLE AND SUBTITLE Comparing a Fischer-Tropsch Alternate Fuel to JP-8 and Their 50-50 Blend: Flow and Flame Visualization Results			5a. CONTRACT NUMBER		
			5b. GRANT NUMBER		
			5c. PROGRAM ELEMENT NUMBER		
6. AUTHOR(S) Hicks, Yolanda, R.; Tacina, Kathleen, M.			5d. PROJECT NUMBER		
			5e. TASK NUMBER		
			5f. WORK UNIT NUMBER WBS 561581.02.08.03.44.01		
7. PERFORMING ORGANIZATION NAME(S) AND ADDRESS(ES) National Aeronautics and Space Administration John H. Glenn Research Center at Lewis Field Cleveland, Ohio 44135-3191			8. PERFORMING ORGANIZATION REPORT NUMBER E-18695		
9. SPONSORING/MONITORING AGENCY NAME(S) AND ADDRESS(ES) National Aeronautics and Space Administration Washington, DC 20546-0001			10. SPONSORING/MONITOR'S ACRONYM(S) NASA		
			11. SPONSORING/MONITORING REPORT NUMBER NASA/TM-2013-217884		
12. DISTRIBUTION/AVAILABILITY STATEMENT Unclassified-Unlimited Subject Category: 07 Available electronically at http://www.sti.nasa.gov This publication is available from the NASA Center for AeroSpace Information, 443-757-5802					
13. SUPPLEMENTARY NOTES					
14. ABSTRACT Combustion performance of a Fischer-Tropsch (FT) jet fuel manufactured by Sasol was compared to JP-8 and a 50-50 blend of the two fuels, using the NASA/Woodward 9 point Lean Direct Injector (LDI) in its baseline configuration. The baseline LDI configuration uses 60° axial air-swirlers, whose vanes generate clockwise swirl, in the streamwise sense. For all cases, the fuel-air equivalence ratio was 0.455, and the combustor inlet pressure and pressure drop were 10-bar and 4 percent. The three inlet temperatures used were 828, 728, and 617 K. The objectives of this experiment were to visually compare JP-8 flames with FT flames for gross features. Specifically, we sought to ascertain in a simple way visible luminosity, sooting, and primary flame length of the FT compared to a standard JP grade fuel. We used color video imaging and high-speed imaging to achieve these goals. The flame color provided a way to qualitatively compare soot formation. The length of the luminous signal measured using the high speed camera allowed an assessment of primary flame length. It was determined that the shortest flames resulted from the FT fuel.					
15. SUBJECT TERMS Optical diagnostics; Combustion; Fuel-air mixing; Alternative fuels; Aircraft gas turbine					
16. SECURITY CLASSIFICATION OF:			17. LIMITATION OF ABSTRACT	18. NUMBER OF PAGES	19a. NAME OF RESPONSIBLE PERSON
a. REPORT	b. ABSTRACT	c. THIS PAGE			STI Help Desk (email:help@sti.nasa.gov)
U	U	U	UU	22	19b. TELEPHONE NUMBER (include area code) 443-757-5802

